

Causes of thermal instability in externally sustained molecular discharges*

William L. Nighan

United Technologies Research Center, East Hartford, Connecticut 06108

(Received 4 October 1976)

In this investigation the basic causes of glow collapse and/or glow-to-arc transition have been examined for convection-cooled, externally sustained molecular-discharge conditions. The results of this analysis show that externally sustained molecular discharges of the type used in CO₂ lasers are inherently unstable. In particular, it is shown that there are two distinct mechanisms which can provide the driving force for thermal instability: (i) electron vibrational excitation leading to a surge in vibrational temperature; and (ii) vibrational reservoir collapse accompanied by a decrease in vibrational temperature. The plasma conditions and basic collisional processes contributing to the occurrence of these thermal instabilities are discussed in detail, with particular emphasis directed toward charged-particle production and loss mechanisms.

I. INTRODUCTION

The use of external, independently controlled ionization sources such as high-energy electron beams and uv radiation as a means of producing relatively uniform, large volume glow discharges at high pressure has resulted in significant advances in gas-discharge technology.¹ With this method of plasma production glow discharges have been produced for molecular laser applications over ranges of pressure and electrical power density which were previously inaccessible as a consequence of the early onset of glow-to-arc transition.

Because of its effectiveness as a means to delay the occurrence of glow collapse, external ionization permits cw glow-discharge operation^{1,2} at pressures of several hundred Torr and above and at electrical power densities in the approximate range 10–1000 W/cm³, conditions exceeding those typical of most self-sustained discharges by a large margin. However, it is because of these high power loadings, coupled with a very high degree of energy nonequilibrium and the absence of effective volumetric energy dissipation mechanisms that plasma instability continues to be a major problem even when external ionization is employed.²⁻⁴

In self-sustained molecular discharges a primary triggering mechanism for thermal instability is the disproportionate response of the electron density to disturbances, owing to the exceptionally strong electron temperature dependence of the ionization rate.⁵ When external ionization is employed to provide a sensibly constant electron production rate, the response of the electron density to disturbances is influenced by a host of complex collision processes, primarily those affecting electron loss.⁶ In addition, electron-molecule energy exchange collisions and processes influencing vibrational energy relaxation assume roles of sig-

nificantly increased importance. For these reasons the factors causing glow collapse and/or arcing in externally sustained discharges are actually more difficult to isolate and understand than is the case for their self-sustained counterparts. The primary purpose of the present paper is identification and interpretation of the basic physical mechanisms leading to instability in externally sustained molecular discharges. Conditions representative of cw, convection cooled CO₂ laser discharges are emphasized in this study. By focusing attention on this well-known system, numerous partially understood characteristics of externally sustained discharges are clarified. These findings should be generally applicable to other high-power-density externally sustained laser discharges as well.

Most of the details of the theoretical formulation utilized in this investigation have been reported previously.⁶⁻⁸ Thus, only the basic elements of the analysis are summarized in Sec. II. Section III has as its objective the development of the physical insight required to understand the causes of *thermal* instability in externally sustained discharges. In this mode of instability temporal changes in neutral particle properties play an important role in the initial growth of disturbances. The evolution of thermal instability is shown to be significantly affected by the nature of the electron loss process, e.g., recombination, attachment, three-body attachment, and by subsequent reactions involving negative ions. Approximate expressions for the growth rate of thermal instabilities under various conditions are presented in order to reveal the causative role of various basic processes. In particular, it is shown that there are at least two distinct mechanisms which can be the driving force for thermal instability in molecular discharges: (i) electron vibrational excitation leading to an increase in vibrational temperature; and (ii) vibrational reservoir collapse

caused by a surge in vibrational-translation relaxation leading to a decrease in vibrational temperature. The conditions required for the occurrence of these thermal instabilities are discussed in detail.

Numerical results are presented in Sec. IV for a variety of specific conditions chosen to be generally similar to those encountered in cw, high-power CO₂ laser discharges. These results show that both the process by which electrons are lost and its dependence on electron temperature exert a very strong influence on the magnitude of the growth rate for thermal instability, even though the predicted steady state may be substantially unaffected. Further, it is shown that thermal stability can be adversely affected by the onset of low energy electron-molecule ionization even when the contribution of this ionization process is only 1% as large as that of the external source. In addition, the results serve to explain how and why negative ions impact on thermal instability when their concentration becomes comparable to that of the electrons.

II. PLASMA ANALYSIS

Rigorous formulation of the criteria for the occurrence of instability considering the several vibrational modes typical of CO₂ laser discharges would be a formidable problem indeed. Here it will be assumed that the discharge contains a single diatomic species in a background of an atomic diluent(s). Rotational-translational equilibrium is assumed to exist at the gas temperature T , and the vibrational energy distribution will be taken as Boltzmann having a vibrational temperature T_v . Thus, the conservation equations for the neutral particle density and the translational and vibrational energy density for a convectively cooled discharge can be expressed⁷

$$\frac{Dn}{Dt} + n\nabla \cdot \vec{U} = 0, \quad (1)$$

$$\begin{aligned} \frac{D}{Dt} (n\mathcal{E}_T) + (n\mathcal{E}_T + P)\nabla \cdot \vec{U} \\ = \kappa \nabla^2 T + \frac{n_m}{\tau_{VT}} [\mathcal{E}_V(T_v) - \mathcal{E}_V(T)] + n_e n (\nu_T/n) k T_e, \end{aligned} \quad (2)$$

$$\begin{aligned} \frac{D}{Dt} (n_m \mathcal{E}_V) + n_m \mathcal{E}_V \nabla \cdot \vec{U} \\ = n_e n (\nu_v/n) k T_e - \frac{n_m}{\tau_{VT}} [\mathcal{E}_V(T_v) - \mathcal{E}_V(T)], \end{aligned} \quad (3)$$

where $D/Dt = \partial/\partial t + \vec{U} \cdot \nabla$, \vec{U} is the mass average velocity of the gas, n and n_m are the total neutral particle number density and molecule density, respectively, κ is the thermal conductivity of the gas, and τ_{VT} is the temperature-dependent time

characterizing vibrational-translational relaxation, i.e., $\tau_{VT}^{-1} = n k_{VT}(T)$, with k_{VT} the rate coefficient for $V-T$ energy relaxation. The average translational-rotational energy per particle, \mathcal{E}_T , is given by

$$\mathcal{E}_T = \left(\frac{3}{2} X_a + \frac{5}{2} X_m\right) k T,$$

where X_a and X_m are the atom and molecule fractional concentrations. In addition, the average vibrational energy per molecule in the present approximation is given by

$$\mathcal{E}_V = \epsilon [\exp(\epsilon/kT_v) - 1]^{-1},$$

where ϵ is the quantum of vibrational energy. Regarding the electron properties, n_e is the electron density, T_e is the generalized (non-Boltzmann) electron temperature,⁵⁻⁸ and ν_v and ν_T are the electron temperature-dependent collision frequencies for vibrational excitation and gas translational heating, respectively.

The corresponding particle conservation equations for electrons and negative ions are written⁷

$$\begin{aligned} \frac{Dn_e}{Dt} + n_e \nabla \cdot \vec{U} + \nabla \cdot (n_e \vec{U}_e) \\ = n_e n k_i - n_e n_p k_r^e - n_e n k_{a_1} - n_e n^2 k_{a_2} + n_n n k_d + n S_E, \end{aligned} \quad (4)$$

$$\begin{aligned} \frac{Dn_n}{Dt} + n_n \nabla \cdot \vec{U} + \nabla \cdot (n_n \vec{U}_n) \\ = n_e n k_{a_1} + n_e n^2 k_{a_2} - n_n n_p k_r^i - n_n n k_d, \end{aligned} \quad (5)$$

where n_n and n_p are the negative-ion and positive-ion number densities ($n_p = n_e + n_n$), \vec{U}_e and \vec{U}_n are the electron and negative-ion drift velocities, and the indicated *mixture weighted* rate coefficients are those for single-step ionization by low energy electrons (k_i), electron recombination (k_r^e), dissociative attachment (k_{a_1}), three-body attachment (k_{a_2}), detachment (k_d), and ion-ion recombination (k_r^i). The quantity S_E represents the electron production rate due to the external source of ionization; generally $n S_E \gg n_e n k_i$ for the conditions of primary interest.

Detailed discussions of the approximations and formulation leading to Eqs. (1)–(5) as applied to this problem are presented elsewhere.⁶⁻⁸ Also, the specific features of the charged-particle collision processes represented in Eqs. (4) and (5), have been discussed in considerable detail.^{8,9}

A. Steady state

Subsonic, convectively cooled discharges are characterized by nearly constant pressure and their one-dimensionality. In addition, convection and volumetric processes dominate over transport phenomena. Thus, the steady-state form of Eqs. (2) and (3) reduces to

$$(nU)C_p \frac{dT}{dx} = \frac{n_m}{\tau_{VT}} [\mathcal{E}_v(T_v) - \mathcal{E}_v(T)] + F_T J E, \quad (6)$$

$$(X_m n U) C_v^v \frac{dT_v}{dx} = F_V J E - \frac{n_m}{\tau_{VT}} [\mathcal{E}_v(T_v) - \mathcal{E}_v(T)], \quad (7)$$

where C_p is the specific heat and where the vibrational specific heat C_v^v is defined as $\partial \mathcal{E}_v / \partial T_v$.⁷ In addition, J is the current density, E is the electric field intensity, and F_T and F_V are the fractional power transfer factors for direct electron translational heating of the gas and electron-molecule vibrational excitation, respectively.¹⁰ In weakly ionized molecular discharges F_T is typically less than 0.1 while F_V is usually greater than 0.5.¹⁰ Thus, Eq. (6) indicates that translational heating of the gas occurs gradually as the gas is convected through the discharge region, primarily as a result of vibrational relaxation. By way of contrast, the vibrational temperature rises very rapidly to a quasiequilibrium value due to the effectiveness of electron-molecule vibrational excitation, with the result that the volumetric terms on the right side of Eq. (7) dominate over the convection term.

Charged-particle properties are dominated entirely by volumetric effects so that the steady-state electron and negative-ion equations are simply Eqs. (4) and (5) with the left sides set equal to zero. However, as will become apparent the complicated interaction among charged-particle loss processes coupled with their great sensitivity to impurities frequently results in considerable uncertainty as to the nature of the processes actually controlling electron and ion loss in specific situations.^{8,9,11-13}

B. Linear stability theory

The equations discussed above can be used to predict conditions favorable for highly efficient electric laser operation for arbitrarily large values of pressure and electric power density. However, in practice the onset of glow collapse or arcing invariably establishes upper limits for these variables, even when external ionization is used to enhance discharge stability. Linear perturbation theory has been shown to be exceptionally

useful as a means for revealing the basic nature of plasma instability in molecular discharges of the type used in laser applications.⁵⁻⁸

In order to evaluate the temporal behavior of small-amplitude disturbances, all plasma properties are considered to be composed of a spatially invariant, steady-state value ψ_0 and a small spatially and temporally varying component $\tilde{\psi}(\vec{x}, t)$ i.e., $\psi(\vec{x}, t) = \psi_0 + \tilde{\psi}(\vec{x}, t)$. The symbol ψ refers to the complete set of variables required to describe the plasma. In addition, the arbitrary local perturbations in plasma properties are represented in the usual way by a superposition of their Fourier components having the form,⁷

$$\Psi_k \exp[i(\omega t - \vec{k} \cdot \vec{x})], \quad (8)$$

where \vec{k} is the wave vector, x is the spatial variable, ω is the complex frequency $\omega_r + i\omega_i$, and Ψ_k is the amplitude of the k th Fourier component of a specific perturbed property, e.g., n_{e_k} , T_{v_k} , \vec{E}_k .

With these considerations providing the basis for the approach to be followed, the complete set of perturbed variables having the form expressed in Eq. (8) is substituted into Eqs. (1)–(5). Numerical experimentation with the resulting system of equations has shown that for the pressures and power densities of interest in externally sustained discharges, local charged-particle transport processes (e.g., ambipolar diffusion) are unimportant compared to volumetric collision processes for disturbance scale sizes (k^{-1}) greater than a few mm. This results in the condition⁶ $\omega_r / \omega_i \ll 1$, so that $i\omega$ in Eq. (8) can be replaced by the disturbance growth rate ν_k . More importantly, in most cw externally sustained discharges the characteristic time for dissipation of acoustic disturbances is much less than the time required for evolution of disturbances in charged particle concentrations and neutral particle properties. For this reason first-order pressure fluctuations are very small⁷ so that the Fourier component of disturbances in neutral density, n_k/n , can be replaced by $-T_k/T$. On the basis of these approximations and after considerable algebraic rearrangement, the following system of first-order equations relating the perturbation amplitudes n_{e_k} , n_{n_k} , T_k , T_{v_k} , and T_{e_k} and the anticipated steady-state properties is obtained:

$$\left(\frac{n_{e_k}}{n_e} + \frac{T_k}{T} \right) \nu_k = - \frac{n_{e_k}}{n_e} \left[\frac{n_n}{n_e} n k_a + \frac{n_e}{n_p} n_p k_r^e + \frac{n}{n_e} S_E \right] + \frac{n_{n_k}}{n_n} \left[\frac{n_n}{n_e} n k_a - \frac{n_n}{n_p} n_p k_r^e \right] - \frac{T_k}{T} \left[n_p k_r^e - \frac{n_n}{n_e} n k_a \hat{k}_a - n^2 k_{a_2} \right] + \frac{T_{e_k}}{T_e} \left[n k_i \hat{k}_i - n_p k_r^e \hat{k}_r - n k_{a_1} \hat{k}_{a_1} - n^2 k_{a_2} \hat{k}_{a_2} \right], \quad (9)$$

$$\left(\frac{n_{n_k} + T_k}{n_n} + \frac{T_k}{T}\right) \nu_k = \frac{n_{e_k}}{n_e} \left[\frac{n_e}{n_n} (nk_{a_1} + n^2 k_{a_2}) - \frac{n_e}{n_p} n_p k_r^i \right] - \frac{n_{n_k}}{n_n} \left[\frac{n_n}{n_p} n_p k_r^i + \frac{n_e}{n_n} (nk_{a_1} + n^2 k_{a_2}) \right] + \frac{T_{e_k}}{T_e} \left[\frac{n_e}{n_n} (nk_{a_1} \hat{k}_{a_1} + n^2 k_{a_2} \hat{k}_{a_2}) \right] - \frac{T_k}{T} \left[n_p k_r^i (1 + \hat{k}_r^i) + nk_d \hat{k}_d + \frac{n_e}{n_n} n^2 k_{a_2} \right], \quad (10)$$

$$\frac{T_k}{T} \nu_k = \frac{T_k}{T} \left[-\frac{\kappa k^2}{nC_p} - (nC_p T)^{-1} [F_V J E (2 - \hat{k}_{VT}) + X_m n^2 k_{VT} C_V^v(T) T + F_T J E] \right] + \frac{T_{v_k}}{T_v} \left[\frac{X_m n^2 k_{VT} C_V^v(T) T}{nC_p T} \right] + \frac{F_T J E}{nC_p T} \left[\frac{n_{e_k}}{n_e} + (1 + \hat{\nu}_T) \frac{T_{e_k}}{T_e} \right]. \quad (11)$$

$$\frac{T_{v_k}}{T_v} \nu_k = \frac{T_k}{T} \left[[X_m n C_V^v(T) T_v]^{-1} [F_V J E (2 - \hat{k}_{VT}) + X_m n^2 k_{VT} C_V^v(T) T - F_V J E] \right] - \frac{T_{v_k}}{T_v} nk_{VT} + \frac{F_V J E}{X_m n C_V^v(T) T_v} \left[\frac{n_{e_k}}{n_e} + (1 + \hat{\nu}_v) \frac{T_{e_k}}{T_e} \right], \quad (12)$$

where ν_k is the growth (or damping) rate of coupled disturbances in n_e , n_n , T , T_v , and T_e .

1. Fractional derivatives of rate coefficients

In Eqs. (9)–(12) the notation \hat{k} (or $\hat{\nu}$) refers to the fractional, or logarithmic, derivative of an electron rate coefficient with respect to electron temperature, i.e.,

$$\hat{k} \equiv \frac{T_e}{k} \frac{\partial k}{\partial T_e} = \frac{\partial \ln k}{\partial \ln T_e}. \quad (13)$$

Thus, \hat{k} is a number, the *magnitude* and *sign* of which are a measure of the sensitivity and nature of the response of a particular process to a small local change in electron temperature. Of course in the case of the gas temperature-dependent rate coefficients such as k_{VT} and k_d this notation refers to the fractional derivative with respect to gas temperature.

2. Electron temperature perturbations

In volume-dominated molecular gas discharges, the characteristic time for electron energy relaxation is very short compared to the time required for the charged particle densities to change,⁶⁻⁸ so that electron energy kinetics respond to a disturbance in an effectively quasisteady manner on the time scale of importance at present. Thus, the first-order quasisteady form of the electron energy equation can be used along with Poisson's equation to obtain a relationship coupling disturbances in electron temperature, electron density and neutral density. It has been shown^{6,7} that the equation relating the perturbation amplitudes T_{e_k} , n_{e_k} , and n_k is

$$\frac{T_{e_k}}{T_e} = \left(\frac{-2 \cos^2 \phi}{1 + \hat{\nu}_u - \hat{\nu}_m \cos 2\phi} \right) \frac{n_{e_k}}{n_e} - \left(\frac{2 \sin^2 \phi}{1 + \hat{\nu}_u - \hat{\nu}_m \cos 2\phi} \right) \frac{n_k}{n} \equiv \left(\frac{-2 \cos^2 \phi}{\hat{\nu}'_u} \right) \frac{n_{e_k}}{n_e} + \left(\frac{-2 \sin^2 \phi}{\hat{\nu}'_u} \right) \frac{n_k}{n}, \quad (14)$$

where ν_u and ν_m are the total electron energy exchange and momentum transfer collision frequencies,^{7,8} respectively, the caret notation referring to logarithmic derivatives of these collision frequencies with respect to electron temperature as described previously. In this equation the angle ϕ is the angle between the direction of the zeroth-order (anticipated steady-state) electric field and the wave propagation vector \vec{k} .

C. Modes of instability

Equations (9)–(12) combined with Eq. (14) can be used to eliminate the perturbation amplitudes n_{e_k} , n_{n_k} , T_k , T_{v_k} , and T_{e_k} . This procedure results in a fourth-order equation for the disturbance growth rate, ν_k , expressed in terms of the *anticipated* steady-state properties of the plasma alone. Each root of this equation can be identified with the initial temporal growth of disturbances of one of the primary time-dependent variables n_e , n_n , T , or T_v . Moreover, it has been shown analytically that for conditions typical of high-power convection discharges in molecular gases, each of the modes of instability represented by solution of Eqs. (9)–(12) can occur.^{5,6,8}

Experimental findings^{6,8,14,15} are in very good accord with theoretical predictions and show that the instabilities which occur are of two distinct types which are manifest in very different ways. Moving striations in CO₂ laser mixtures have been observed in both self-sustained⁸ and externally sustained discharges.¹⁵ This manifestation of instability is a consequence of the coupling between electron and negative-ion production and is referred to as *attachment instability*.^{6,14,15} This instability does not depend explicitly on discharge power density. By way of contrast, plasma constriction and/or glow collapse is always found to depend on electric power density. For this reason this type of instability has very important conse-

quences in high-power lasers. The causes of glow collapse are not as well understood as those of attachment instability. However, both theory and experiment suggest that this mode is of the thermal type.^{5-7,16-20}

III. THERMAL INSTABILITY

A. Nature of thermal instability in molecular discharges

The occurrence of thermal instability is a direct consequence of the highly nonequilibrium state characterizing weakly ionized molecular discharges. In such discharges the energy per particle characterizing electron translation, vibrational excitation, and neutral particle translation differs greatly, i.e., $T_e > T_v > T$. In laser applications it is precisely this circumstance that permits efficient conversion of electrical energy to vibrational energy and ultimately to infrared radiation. Indeed, the steady-state plasma conditions required to ensure the efficiency of this process are generally well understood. What are not well understood are the many different ways the anticipated steady state can respond to a disturbance.

Figure 1 provides a qualitative illustration of the sequence of events accompanying a local, constant pressure disturbance in the diatomic gas discharge under consideration.^{5,6} As indicated, the local decrease in gas density in response to a gas temperature perturbation leads to an effectively instantaneous increase in electron temperature. Equation (14) shows that the electron temperature disturbance will be largest in the direction normal to the steady electric field ($\phi = 90^\circ$). In a self-sustained discharge (without negative ions) there would result a disproportionately large

increase in the electron density in this direction due to the strong electron temperature dependence of the ionization rate coefficient (i.e., $\hat{k}_i \gg 1$). Use of an external source of ionization is intended to substantially eliminate this effect by providing an electron production rate which is sensibly independent of plasma disturbances. In this case the electron density disturbance is determined by the nature and electron temperature dependence of the electron loss process which is not under control. Thus, while the magnitude of the electron density response to a disturbance is greatly reduced when external ionization is employed, the response of the electron density to an increase in T_e can be either positive or negative as indicated in the figure because of the variable nature of electron loss mechanisms. Electron molecule vibrational excitation (process 1 in Fig. 1) is influenced by changes in both electron temperature and electron density, and vibrational energy relaxation (process 3) is dependent on gas-temperature changes. With the vibrational temperature maintained in quasiequilibrium between T_e and T at a level determined by the competing influences of electron excitation and neutral particle collisional relaxation, it is clear that the response of T_v to a disturbance can be either positive or negative in externally sustained discharges, depending on a host of simultaneously occurring processes. Thermal instability will result when the collisional feedback mechanisms indicated in the figure reinforce one or more elements of this sequence during a disturbance.

B. Electron-molecule vibrational power transfer

The results presented in Sec. IV will show that the driving force for thermal instability in molecular discharges is frequently provided by the response of electron-molecule vibrational excitation processes to a disturbance in medium properties (process 1 in Fig. 1). This represents a significant distinction between molecular and atomic discharges. In order to assess the nature of this response and its dependence on plasma variables, it is useful to examine the electron-molecule vibrational power transfer term in Eq. (3). Comparison of Eqs. (3) and (7) shows that the electron-molecule vibrational energy transfer may be expressed in the form

$$F_v J E \equiv P_v = n_e n (v_v/n) k T_e. \quad (15)$$

Linear perturbation theory can be used to determine an expression relating the first-order disturbance in vibrational excitation P_{v_k} to the Fourier components of perturbed quantities. In the absence of acoustic disturbances, the resulting equation is easily shown to be

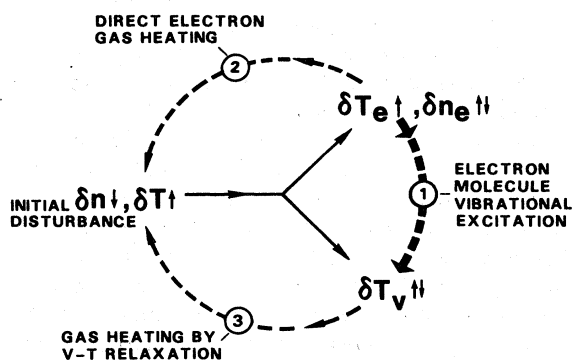


FIG. 1. Illustration of the sequence of events accompanying a local constant pressure disturbance in a diatomic gas discharge. The direct coupling of perturbations in neutral density and temperature to the electronic and vibrational properties of the gas is indicated by solid lines, while the subsequent feedback processes are indicated by dashed lines.

$$\frac{P_{v_k}}{P_v} = \frac{n_{e_k}}{n_e} - \frac{T_k}{T} + (1 + \hat{\nu}_v) \frac{T_{e_k}}{T_e}. \quad (16)$$

When the discharge is self-sustaining the electron density disturbance (n_{e_k}/n_e) in the direction normal to the steady electric field direction completely dominates this expression, with the result that the electron-molecule vibrational excitation process increases sharply in this direction in response to a disturbance in gas temperature, e.g., for $\phi \sim 90^\circ$, $P_{v_k}/P_v \approx 10(T_k/T)$. When external ionization is employed to suppress the influence of the electron-temperature-dependent ionization rate, the electron density disturbance no longer dominates Eq. (16). In this case the direct effect on vibrational excitation of the electron-temperature and gas-temperature disturbances become very important. By using Eq. (14) to express the electron-temperature disturbance in terms of the disturbances in electron density and neutral density, Eq. (16) becomes

$$\begin{aligned} \frac{P_{v_k}/P_v}{T_k/T} = & -1 + \frac{2 \sin^2 \phi (1 + \hat{\nu}_v)}{1 + \hat{\nu}_u - \hat{\nu}_m \cos 2\phi} \\ & + \frac{n_{e_k}/n_e}{T_k/T} \left(1 - \frac{2 \cos^2 \phi (1 + \hat{\nu}_v)}{1 + \hat{\nu}_u - \hat{\nu}_m \cos 2\phi} \right). \end{aligned} \quad (17)$$

When the electron vibrational energy transfer factor F_v is near unity ($\nu_v \approx \nu_u$) as is often the case in molecular discharges,¹⁰ and when the electron-temperature dependence of the energy exchange collision frequency is strong ($\hat{\nu}_u \approx \hat{\nu}_v \gg \hat{\nu}_m$), Eq. (20) can be simplified considerably for illustrative purposes i.e.,

$$\frac{P_{v_k}/P_v}{T_k/T} \approx -1 + 2 \sin^2 \phi + \frac{n_{e_k}/n_e}{T_k/T} (1 - 2 \cos^2 \phi). \quad (18)$$

For an externally sustained, recombination dominated plasma Eq. (9) can be used to show that the ratio $(n_{e_k}/n_e)(T_k/T)^{-1}$ is approximately $-\frac{1}{2}$ if the electron density response is nearly quasisteady,^{6,7} and if the electron recombination coefficient is independent of electron temperature. A negative value of $(n_{e_k}/n_e)(T_k/T)^{-1}$ implies that a local temperature increase results in a decrease in electron density due to the accompanying decrease in neutral density. Using a value of $-\frac{1}{2}$ for $(n_{e_k}/n_e)(T_k/T)^{-1}$, Eq. (18) can be used to show that the fractional change in electron vibrational excitation relative to a change in gas temperature is anisotropic as expected, varying from $-\frac{1}{2}$ for $\phi = 0^\circ$ to $\frac{1}{2}$ for $\phi = 90^\circ$. In contrast to the situation typical of self-sustained discharges, the relative magnitude of the change in vibrational excitation is of the same order as that of the change in gas temperature, e.g., for $\phi \sim 90^\circ$, $P_{v_k}/P_v \sim T_k/T$.

It should be pointed out that the uncertainty introduced by the approximations permitting elimination of the explicit dependence of Eq. (17) on $\hat{\nu}_u$, $\hat{\nu}_v$, and $\hat{\nu}_m$ is far less than that associated with the illustrative choice of simple recombination as the electron loss mechanism, i.e., $(n_{e_k}/n_e)(T_k/T)^{-1} = -\frac{1}{2}$. The next section will show that the magnitude of the disturbance in electron-molecule vibrational energy transfer is very sensitive to the nature of the electron loss process. This sensitivity is a consequence of the fact that the fractional change in electron density relative to a change in gas temperature is reduced by an order of magnitude or more because of the effectiveness of the external ionization source, with the result that the fractional response to a disturbance of many processes passes through zero as the conditions of interest vary.

C. Electron loss processes

Frequently the growth rate of thermal disturbances is much smaller than the rates influencing electron production and loss. When this is the case the electron response is nearly quasisteady so that to a reasonable approximation the left side of Eq. (9) can be neglected relative to the terms on the right side. This approximation assists in developing insight regarding the factors which influence electron density perturbations in externally sustained discharges. By using Eq. (14) to express the electron temperature perturbations in terms of the perturbations in electron and gas density the fractional electron density disturbance required for evaluation of Eq. (17), can be obtained.

For molecular plasmas such that the principal volumetric electron loss process is either recombination, dissociative attachment, or three-body attachment, respectively,^{8,9} the quasisteady electron density disturbances relative to temperature disturbances are easily obtained using Eqs. (9) and (14), i.e.,

recombination:

$$\frac{n_{e_k}/n_e}{T_k/T} = -\frac{1}{2} \frac{(1 + 2 \sin^2 \phi \hat{k}_r^e / \hat{\nu}'_u)}{(1 - 2 \cos^2 \phi \hat{k}_r^e / \hat{\nu}'_u)}, \quad (19)$$

dissociative attachment:

$$\frac{n_{e_k}/n_e}{T_k/T} = \frac{-2 \sin^2 \phi \hat{k}_{a_1} / \hat{\nu}'_u}{1 - 2 \cos^2 \phi \hat{k}_{a_1} / \hat{\nu}'_u}, \quad (20)$$

three-body attachment:

$$\frac{n_{e_k}/n_e}{T_k/T} = \frac{1 - 2 \sin^2 \phi \hat{k}_{a_2} / \hat{\nu}'_u}{1 - 2 \cos^2 \phi \hat{k}_{a_2} / \hat{\nu}'_u}. \quad (21)$$

These equations show that the relative electron density response to a change in gas temperature is affected by the following factors: the particular

process by which electrons are lost; the electron temperature dependence of the loss process as reflected by the magnitude and sign of the fractional derivative, \hat{k} ; and by spatial orientation reflecting the nature of the coupling between disturbances in T_e , n_e , and n [Eq. (14)]. It is generally found that an increase in electron density in response to an increase in temperature favors further growth of thermal disturbances, i.e., thermal instability. Thus, based on examination of Eqs. (19)–(21) the following general observations can be made: (1) Even if the electron temperature dependence of the process by which electrons are lost is small ($\hat{k} \sim 0$) with the result that the electron density disturbance is isotropic, the specific process by which electrons are lost significantly influences the nature and magnitude of the first-order electron density disturbance. Note that if \hat{k} is set equal to zero in each of Eqs. (19)–(21) $(n_{e_k}/n_e)(T_k/T)^{-1}$ increases from $-\frac{1}{2}$ to 0 to $+1$ for recombination, attachment, and three-body attachment as the primary electron loss processes, respectively. Using Eq. (18) it is easy to show that the fractional change in the electron-molecule vibrational excitation process in the direction normal to the electric field ($\phi = 90^\circ$) varies from $\frac{1}{2}$ to 1 to 2 in response to such changes in the electron density disturbance. In Sec. IV the thermal instability growth rate will be shown to increase by about an order of magnitude in response to such changes in the electron loss process, with a recombination-dominated plasma being the most stable. (2) An electron loss process having a rate coefficient which is a decreasing function of electron temperature ($\hat{k} < 0$) favors an increase in $(n_{e_k}/n_e)(T_k/T)^{-1}$, the stronger the electron temperature dependence the larger the effect. (3) Given a particle loss process having a strong dependence on electron temperature, the electron energy exchange factor $\hat{\nu}'_u$ can exert an important influence by way of its effect on the magnitude of the electron temperature disturbance. Equation (14) shows that there exists an electron temperature inertial effect tending to minimize the magnitude of T_{e_k} if the energy exchange collision frequency is a strong function of electron temperature, i.e., $|\hat{\nu}'_u| \gg 1$. This in turn tends to reduce the magnitude of electron density disturbances as the form of Eqs. (19)–(21) indicates.

D. Approximate instability growth rate

Quantitative determination of the growth (or damping) rates for disturbances requires self-consistent solution of the fourth-order set of Eqs. (9)–(12), the results of which are presented in the next section. However, it has been found that

there are two distinctly different mechanisms which can lead to thermal instability in externally molecular discharges. Consideration of approximate expressions for the growth rates of thermal disturbances in these two limits facilitates understanding of the numerical data to be discussed in the next section.

1. Electron-driven vibrational mode

On the basis of numerical experimentation it has been found that for a host of conditions of importance to externally sustained molecular discharges only one root resulting from solution of Eqs. (9)–(12) is unstable, i.e., $\nu_k > 0$. This indication of instability is readily identified with an increase in electron-molecule vibrational excitation during a disturbance resulting in an increase in T_v (Fig. 1). As might be expected on the basis of the discussion in previous paragraphs, it is found that the maximum growth rate for disturbances occurs in the direction normal to the steady field ($\phi = 90^\circ$) for which disturbances in gas density (temperature) and electron temperature are strongly coupled [Eq. (14)]. To a reasonable degree of approximation the growth rate for this electron-driven vibrational mode may be expressed,

$$\nu_k \sim \frac{JE}{nC_p T} \frac{P_{v_k}/P_v}{T_k/T} \quad (22)$$

Using Eq. (18) to express the fractional disturbance in vibrational power transfer in terms of the fractional electron density disturbance, Eq. (22) becomes

$$\nu_k \sim \frac{JE}{nC_p T} \left(1 + \frac{n_{e_k}/n_e}{T_k/T} \right), \quad \phi \sim 90^\circ \quad (23)$$

Clearly, the growth rate increases with electrical power density as anticipated. More importantly, with the minimum value of $(n_{e_k}/n_e)(T_k/T)^{-1}$ for a recombination dominated plasma equal to $-\frac{1}{2}$, the criterion for instability ($\nu_k > 0$) is always satisfied at the power density levels of importance in molecular laser applications. The importance of the relatively small changes in the electron density disturbance [Eq. (19)–(21)] is readily apparent from the form of Eq. (23). For example, as $(n_{e_k}/n_e)(T_k/T)^{-1}$ varies from $-\frac{1}{2}$ to 0 to 1, values typical of recombination, attachment, and three-body attachment loss, respectively, the magnitude of the growth rate at constant power density increases by a factor of 4. Of course, the electron temperature dependence of the rate coefficient for the loss process also exerts a significant influence on $(n_{e_k}/n_e)(T_k/T)^{-1}$ for reasons discussed previously.

2. Vibrational relaxation mode

The conditions for the occurrence of this mode are identified in Sec. IV, which shows that the growth rate is nearly isotropic since electron properties are not directly involved. To a first approximation the criterion for growth of the V - T energy relaxation mode may be expressed,

$$\nu_k \sim - \left(\frac{1}{\tau_{VT}} + \frac{JE}{nC_p T} (2 - \hat{k}_{VT}) \right) > 0. \quad (24)$$

Recall, that \hat{k}_{VT} is the fractional derivative of the V - T rate coefficient with respect to gas temperature, e.g., if $k_{VT} \sim T^4$ then $\hat{k}_{VT} = 4$. Since τ_{VT} is positive the first term in this equation is always negative, i.e., stabilizing, while the second term will be positive if $\hat{k}_{VT} > 2$. The form of this equation shows that there are two significant factors influencing this mode of instability¹⁷: (1) the degree of V - T nonequilibrium as determined by the value of τ_{VT} and (2) the temperature dependence of the V - T rate coefficient. For a specific value of electrical power density JE , the higher the value of τ_{VT} the greater the difference between T_v and T and the smaller the stabilizing term in Eq. (24). Moreover, a high degree of nonequilibrium between vibration and translation (τ_{VT} large, $T_v \gg T$) coupled with a V - T rate coefficient having a strong positive dependence on gas temperature ($\hat{k}_{VT} > 2$) can lead to a collapse of the vibrational energy reservoir accompanied by a sharp decline in T_v . This phenomenon is not directly affected by the external ionization source since specifics of charged-particle production and loss are not involved.

IV. NUMERICAL RESULTS AND DISCUSSION

The approximate expressions discussed in the previous section for the electron driven and vibrational relaxation modes of thermal instability show that the instability growth rate increases with increasing electrical power density at constant pressure. In cw electric laser applications efficient vibrational excitation and maintenance of adequate gain require sensibly constant values of fractional ionization (n_e/n), electron temperature (as determined by E/n), and gas temperature. These factors combine in such a way that the electric power density scales approximately as the square of the pressure. Thus, increases in pressure are usually accompanied by somewhat disproportionately larger increases in power density. For these reasons the approximate expressions given by Eqs. (23) and (24) indicate that the growth rate of thermal disturbances increases with increasing pressure and/or power density.

However, the leverage factors which multiply

the anticipated steady-state power density, $(P_{v_k}/P_v)(T_k/T)^{-1}$ for the electron driven mode and $(2 - \hat{k}_{VT})$ for the vibrational relaxation mode, are subject to large variation with changes in either pressure or power density. The nature of these variations is often highly uncertain. For this reason emphasis in the present study has been placed on quantitative evaluation of the effect on instability growth rates of variations in electron production and loss processes and in vibrational relaxation.

A. Basic considerations

The present diatomic gas model can be used as a reasonable representation of CO₂ laser mixtures containing N₂ and He by assuming⁶ (i) that the CO₂ asymmetric stretch and N₂ vibrational modes constitute a single vibrational level at a temperature T_v , and that these modes remain coupled during a disturbance, and (ii) that the CO₂ symmetric stretch mode, the CO₂ bending mode, and all rotational levels of CO₂ and N₂ are in equilibrium at the gas translational temperature T . Consistent with this approximation, vibration-translation relaxation is considered to occur by way of the V - V process $\text{CO}_2(001) + M \rightarrow \text{CO}_2(lm0) + M$. Also, the collision frequency ν_v refers to the combined vibrational excitation of N₂ and the CO₂ asymmetric stretch mode, while ν_T includes the cumulative effect of all electron processes resulting in gas heating, i.e., elastic collisions, rotational excitation, and excitation of the CO₂ symmetric stretch and bending modes.^{5,6}

Figure 2 presents electron collision frequencies computed on the basis of this model for a CO₂-N₂-He laser mixture. The factors influencing the magnitude and electron temperature dependence of these data are well understood and are found to be generally similar for a variety of gas mixtures in which either N₂ or CO vibrational excitation dominates electron-molecule energy exchange.¹⁰ The fractional derivatives [Eq. (13)] of these collision frequencies are presented in Fig. 3. Although $\hat{\nu}_v$ is approximately equal to $\hat{\nu}_T$ over much of the range covered as assumed previously in connection with the development leading to Eq. (18), the data show very large variations in the region of electron temperature for which vibrational excitation is very efficient ($F_v > 0.5$). When external ionization is employed the entire range of electron temperature shown in Fig. 3 is accessible, unlike the case for self-sustained discharges which require sensibly constant electron temperature ($T_e \sim 1$ eV).⁸

Plasma conditions

Numerical experimentation with various commonly used CO₂ laser mixtures has shown that the

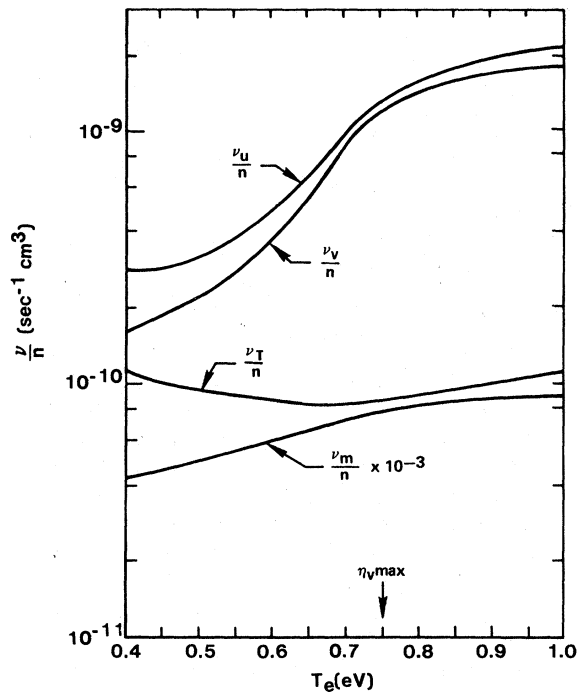


FIG. 2. Electron-molecule collision frequencies for total energy transfer ν_u , vibrational excitation ν_v , translational-rotational gas heating ν_T , and momentum transfer ν_m , computed for a CO_2 - N_2 - He mixture in the number density proportions 0.05-0.35-0.60. These data are not unduly sensitive to reasonable variations in mixture proportions over the electron temperature range indicated. η_v max indicates the T_e value for which vibrational excitation is most efficient.

fractional derivatives presented in Fig. 3 are not substantially altered by mixture changes for N_2 : CO_2 number density ratios in the 2 to 10 range. This follows as a consequence of the dominant role played by N_2 vibrational excitation in CO_2 laser mixtures. Thus, in the examples to follow the CO_2 - N_2 - He gas mixture was fixed in the proportions 0.05:0.35:0.60. The electron temperature dependent rate coefficients for this mixture have been discussed in considerable detail elsewhere.^{8,10} Certain other conditions typical of cw convection cooled discharges were also held constant at the following values: discharge inlet velocity, 100m/sec; inlet temperature, 300°K; and pressure, 0.25 atm. Values of the applied electric field were chosen so as to yield E/n values corresponding to efficient electron energy transfer to the coupled $\text{N}_2(v=n)$ - $\text{CO}_2(00n)$ modes, i.e., at the discharge entrance $E/n_0 \sim 1 \times 10^{-16}$ V cm²; for this gas mixture the corresponding electron temperature and fractional vibrational power transfer values are approximately 0.65 eV and 0.9, respectively. In addition, the external ionization

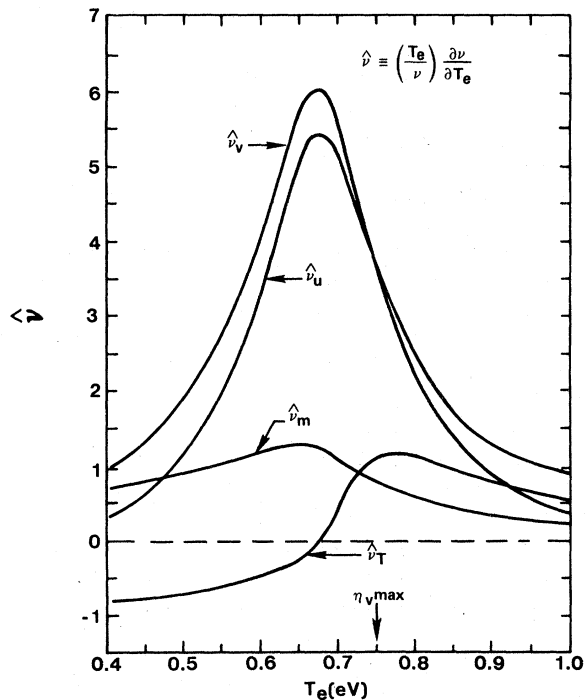


FIG. 3. Fractional derivatives of the electron collision frequency data presented in Fig. 2. Values of $|\hat{\nu}| < 1$ imply a relatively weak dependence on electron temperature.

source function (S_E) was set at a value of 10^{-3} sec⁻¹. These conditions result in values of electron density and electrical power density at the discharge inlet of approximately 3×10^{11} cm⁻³ and 100 W/cm³, respectively. Under such circumstances the plasma behavior is indeed dominated by volume processes. It is worth emphasizing that once the ranges of steady-state plasma properties such as pressure, gas mixture, electron temperature, electron density, and electrical power density have been established, thermal instability is far more sensitive to specific microscopic details of electron production and loss processes than to variations in macroscopic plasma conditions.

B. Effect of variations in the electron loss mechanism

There is always considerable uncertainty as to the precise nature of electron loss for conditions typical of high-pressure electric lasers.^{6,8,9} Even when it is anticipated that the electron loss should be dominated by dissociative recombination, analysis of the dependence of the discharge current density in terms of the intensity of the external ionization source and the applied electric field often indicates that attachment is the principal loss mechanism. At total pressures above about

0.1 atm, O_2 fractional concentrations as low as 10^{-3} can lead to electron loss by way of the well-known three-body attachment process $e + O_2 + M \rightarrow O_2^- + M$.^{21,22} Moreover, because the precise species of ions^{12,13} and low-level impurity concentrations^{8,9,11} are generally unknown, the electron temperature dependence of the electron loss process cannot be determined. These major uncertainties in charged-particle kinetics have relatively little effect on the anticipated steady state, many aspects of which are dominated by electron molecule vibrational excitation. Since the fractional power consumed by the ionization process in molecular discharges is usually insignificant¹⁰ (~ 0.01 – 0.1%), variations in the electron loss process are relatively easily compensated for by way of changes in the external ionization source which can be adjusted until the desired electron density is obtained.

1. Spatial variation of plasma properties

To assess the effect of different electron loss processes in CO_2 laser mixtures three basic conditions were examined. These included electron loss dominated by (1) recombination, (2) dissociative attachment, and (3) three-body attachment. The magnitudes of the rate coefficients for these processes, k_r^e , k_{a1} , and k_{a2} , were selected so as to yield essentially the same electron density for a given value of the external source, using a reference value⁸ of $6 \times 10^{-8} \text{ sec}^{-1} \text{ cm}^3$ for k_r^e at an electron temperature of 1.0 eV. The electron temperature dependence of the loss coefficients could then be varied with little change in the steady state properties.

Figure 4 presents computed variations in the direction of flow of the steady state properties T , T_v , T_e , and n_e for the various electron loss processes examined. As a consequence of the decreasing gas density accompanying the rise in gas temperature, there is an increase in E/n and therefore T_e with axial location as shown. The axial variation in electron density (and therefore current density) for the cases shown in the figure reflects both the changing neutral density and the electron temperature dependence of the electron loss rate, the details of which will be discussed subsequently. However, the change in steady-state properties reflecting the various electron loss processes are relatively small and are well within the range of typical experimental variation. For example, at the discharge inlet ($x=0$) the electrical power density is within a few percent of 100 W/cm^3 for each of the cases considered, while the power density averaged over the first 10 cm of the discharge varies from approximately 105 W/cm^3 for

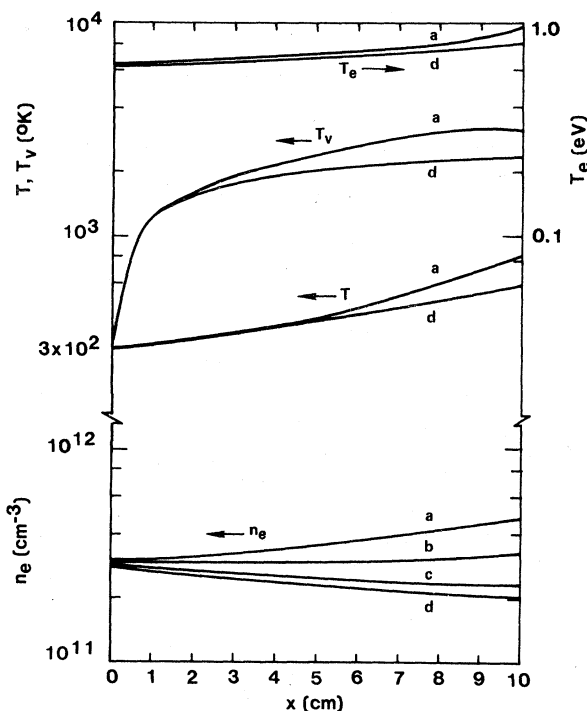


FIG. 4. Computed variation of steady-state properties in the direction of flow for typical convection discharge conditions: $p = 0.25 \text{ atm}$; $T_0 = 300 \text{ °K}$ and $U_0 = 100 \text{ m/sec}$. The external source function S_E was held constant at 10^{-3} sec^{-1} . The vibrational temperature T_v refers to the coupled $CO_2(00n)-N_2(v)$ systems for a CO_2-N_2-He (0.05–0.35–0.60) mixture as described in Sec. IV. The data shown were obtained considering as the electron loss process: three-body attachment with $\hat{k}_{a2} = -\frac{3}{2}$ (curve a); dissociative attachment with $\hat{k}_{a1} = -\frac{3}{2}$ (curve b); dissociative recombination with $\hat{k}_r^e = -\frac{3}{2}$ and $-\frac{1}{2}$ (curves c and d).

the recombination dominated plasmas [cases (c) and (d)] to 180 W/cm^3 for the three-body attachment case (a); the latter increase reflecting the stronger dependence of the electron density on changes in gas density when three-body attachment is taken as the loss process.

2. Computed thermal instability growth rates

In order to determine disturbance growth rates for the conditions of Fig. 4, Eqs. (9)–(12) were numerically solved for various values of the wave vector \vec{k} , i.e., k and ϕ were varied parametrically. For values of k^{-1} greater than a few mm the computed values of ν_k were found to be insensitive to the magnitude of the wave vector indicating that local transport processes are ineffective at damping medium disturbances for the conditions of interest. Thus, all subsequent discussion of growth

rates will refer to "long-wavelength" disturbances, i.e., $k^{-1} \gtrsim 3$ mm. Variation of the direction (ϕ) of \vec{k} relative to the steady electric field was found to significantly affect the computed growth rates as anticipated. Indeed, all four roots resulting from solution of Eqs. (9)–(12) were found to be negative for $\phi = 0^\circ$ indicative of damping of disturbances in all time dependent properties. For values of ϕ greater than about 50° a single positive root appeared, the magnitude of which increased significantly with angle reaching a maximum value for $\phi = 90^\circ$. This positive root is readily identified with the electron driven vibrational mode of thermal instability discussed in Sec. III.

Unlike the anticipated steady-state characteristics, the computed growth rates for thermal instability were found to vary greatly with changes in the electron loss process. Figure 5 presents the computed growth rates for the electron driven mode of thermal instability corresponding to cases (a)–(d) in Fig. 4. Because of the nature of the coupling between disturbances in T_e and n [Eq. (14)], the growth rate is found to have its maximum value in the direction normal to the electric field; the value of ν for $\phi = 90^\circ$ is shown in the figure. These data show the effects of both the

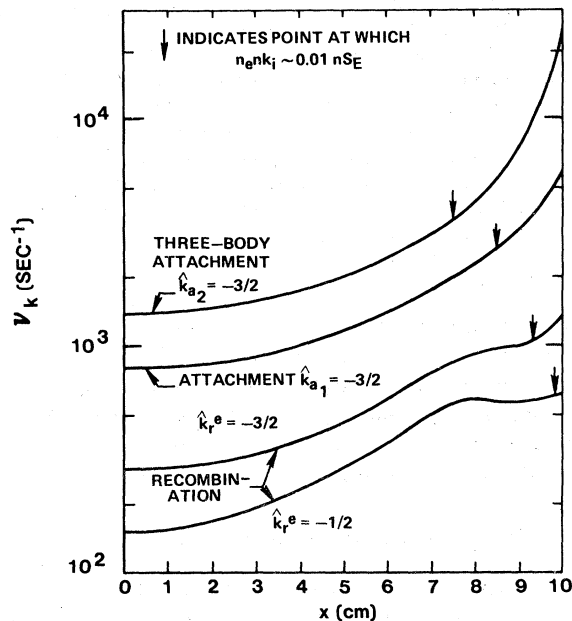


FIG. 5. Computed instability growth rate in the direction normal to the steady electric field ($\phi = 90^\circ$) corresponding to the conditions of Fig. 4. The electrical power density throughout the first several centimeters is approximately 100 W/cm^3 for all cases. The arrow in this and all subsequent figures indicates the spatial location at which the contribution of avalanche ionization to the total electron production is approximately 1%.

electron temperature dependence of the electron loss rate and the effect of changes in the loss process itself. When recombination was considered as the electron loss mechanism [cases (c) and (d)] the growth rate was found to increase by approximately a factor of 2 as the electron temperature variation of k_r^e was changed from $T_e^{-1/2}$ to $T_e^{-3/2}$, i.e., $\hat{k}_r^e = -\frac{1}{2}$ and $\hat{k}_r^e = -\frac{3}{2}$ [Eq. (13)]. More importantly, by choosing an electron temperature dependence of $T_e^{-3/2}$ for the rate coefficient of each loss process ($\hat{k}^e = -\frac{3}{2}$), the growth rate was found to increase by a factor of about 5 as the loss process was changed from recombination to attachment to three-body attachment, a result consistent with the discussion of Sec. III.

Figure 5 also shows a significant increase in the instability growth rate in the flow direction for all cases. This reflects the effect of increasing gas temperature which in turn results in an increase in the V - T relaxation rate which provides the primary feedback path leading to enhanced gas heating (process 3 in Fig. 1). Of particular significance is the fact that when the electron temperature rises due to the increase in E/n with position, a downstream location is reached where the growth rate begins to rise very rapidly ($x \sim 8$ – 10 cm in this example). This corresponds to the point at which the ionization due to low-energy electron-molecule impact first becomes significant during a disturbance. Moreover, this effect becomes important when the steady-state contribution of low-energy electron-molecule ionization is only about 1% of that due to the external source (this point is indicated by an arrow in the figure). Thus, it can be concluded that because of the exceptionally strong dependence of the ionization rate coefficient on electron temperature ($\hat{k}_i > 10$), avalanche ionization affects thermal stability for conditions such that the steady state would be almost entirely unaffected.

3. Electron density disturbances

The trends exhibited by the data of Fig. 5 are entirely consistent with expectations based on the change in the electron density response to a disturbance as the electron loss process varies as discussed in Sec. III. Figure 6 presents the computed spatial variation of the fractional electron density disturbance, $(n_{eR}/n_e)(T_R/T)^{-1}$, corresponding to the growth rates of Fig. 5. These data show that an increasingly negative electron temperature dependence of the loss coefficient increases the magnitude of the electron density disturbance as expected. Note that as \hat{k}_r^e is varied from $-\frac{1}{2}$ to $-\frac{3}{2}$, $(n_{eR}/n_e)(T_R/T)^{-1}$ increases from a value of approximately -0.5 to a value of about -0.3 , a trend consistent with Eq. (19). Further increases

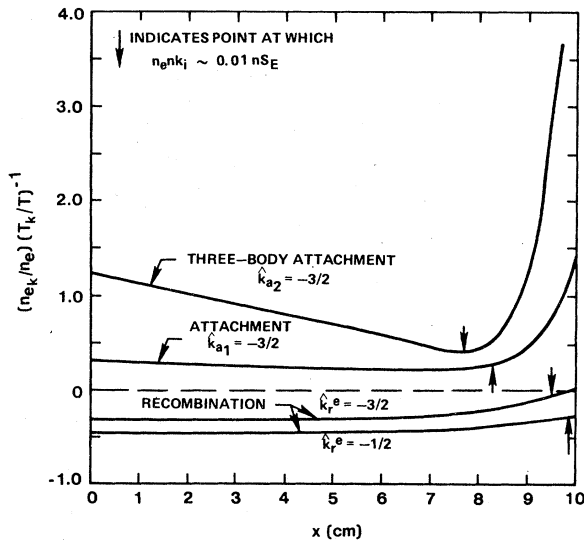


FIG. 6. Computed fractional electron density disturbance relative to a disturbance in gas temperature corresponding to the thermal instability growth rates of Fig. 5.

in the magnitude of the electron density disturbance occur in accordance with the predictions of Eq. (20) and (21) as the loss process is changed from recombination to attachment while retaining the same *negative* electron temperature dependence, i.e., $\hat{k} = -\frac{3}{2}$. Note that the quantity $(n_e/n_e)(T_k/T)^{-1}$ actually changes from negative to positive as the loss process changes from recombination to attachment. Examination of Eq. (23) and consideration of the accompanying discussion serve to explain why the resulting impact on the instability growth rate is so large.

The effect of the onset of avalanche ionization on the fractional electron density disturbance is particularly pronounced for the attachment-dominated plasma in which a slightly higher electron temperature is reached before the end of the discharge region. However, the increasing trend in $(n_e/n_e)(T_k/T)^{-1}$ caused by low-energy electron-molecule ionization is also apparent for the recombination dominated plasma even for positions to the left of the arrow for which the predicted steady-state contribution of avalanche ionization is less than 1% of that of the external source. This indicates that the thermal instability growth rate can tend toward the value typical of self-sustained plasmas even if the net contribution from avalanche ionization is as low as 1% of that due to the external source, a condition likely to be first reached in the higher temperature (low density) regions near boundary layers and electrodes.

4. Plasma residence time

As elaborated upon elsewhere^{2,5,6} an apparently stable (i.e., diffuse) convection discharge of the type under consideration can be maintained until local conditions reach the point such that the time characterizing the growth of thermal disturbances, ($\tau_k \equiv \nu_k^{-1}$), becomes comparable to or less than the remaining residence time of the plasma in the discharge region. Computations of the thermal instability growth time for a *self-sustained* discharge under conditions otherwise the same as those of Fig. 5 have shown that τ_k is well below 10^{-3} sec for all locations in a recombination-dominated discharge, and below 10^{-4} sec when dissociative attachment was considered as the electron loss. Thus, with an inlet flow velocity of 100 m/sec it is to be expected that a diffuse, self-sustained discharge could be maintained for the pressures (~ 0.25 atm) and power densities (~ 100 W/cm³) of the present example only if the discharge were very short in the flow direction, e.g., less than 10 cm.

The results of Fig. 5 show that the growth time τ_k can be on the order of 10^{-3} sec or less even when external ionization is employed. Indeed the magnitude of the thermal instability growth rate has been shown to be very sensitive to the nature of the electron loss process. While utilization of external means of plasma production permits substantial increases in the pressure and power density attainable in subsonic convection discharges, the results presented in Fig. 5 indicate that the magnitude of the instability growth rate will limit the practical flow length of such discharges to values in the 10–20-cm range, and perhaps even less.

C. Variations in the attachment coefficient

Although the exact electron temperature dependence of the recombination coefficient k_r^e must be considered unknown for the present conditions, generally k_r^e will have a relatively weak negative dependence on electron temperature,²³ i.e., $-2 < \hat{k}_r^e < 0$. However, the electron temperature dependence of the rate coefficient for dissociative attachment can vary substantially⁸ and is frequently a strong positive function of electron temperature. Such is the case for dissociative attachment of CO₂ or O₂, for example, both species having \hat{k}_{a1} values much greater than unity.⁸ A positive electron temperature dependence for the electron attachment rate should exert a stabilizing influence on the electron driven thermal mode by causing a reduction in electron density in response to an increase in neutral temperature as indicated by the form of Eq. (20) with $\phi = 90^\circ$. However, it is now

well known^{8,14,15} that such a variation of the attachment rate coefficient ($\hat{k}_{a_1} > 0$) can lead to *attachment instability* as discussed in Sec. II. The growth rate for this mode of instability is positive only in the direction of the electric field ($\phi = 0^\circ$), a condition favoring plasma striation rather than glow collapse.^{8,15} Therefore, with $\hat{k}_{a_1} > 0$ the situation is particularly complicated with more than one class of instability expected, i.e., more than one positive root may result upon solution of Eqs. (9)–(12). Furthermore, with k_{a_1} a strong, positive function of electron temperature, recombination may be the dominant electron loss mechanism at the discharge inlet where T_e and k_{a_1} are low, with attachment dominating at some point downstream as k_{a_1} increases with T_e .

Figure 7 shows the computed instability growth rates for the same general conditions at the discharge entrance as those corresponding to case *c* in Figs. 5 and 6. However, in addition to electron loss due to recombination ($\hat{k}_r^e = -\frac{3}{2}$), dissocia-

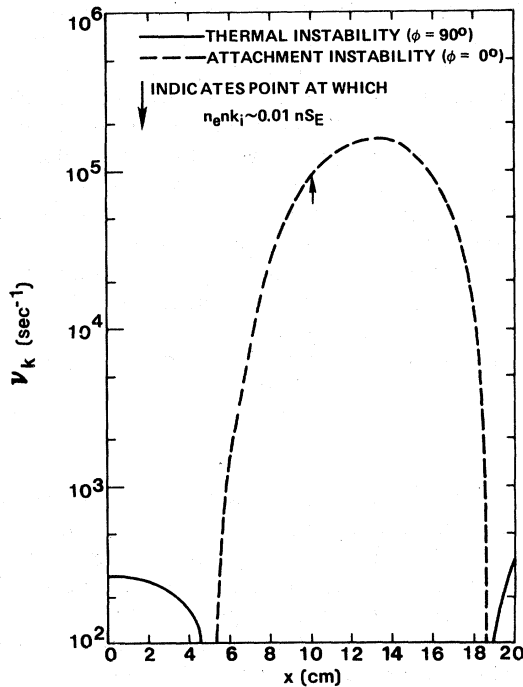


FIG. 7. Computed growth rates for thermal instability ($\phi = 90^\circ$) and attachment instability ($\phi = 0^\circ$) for conditions generally similar to those of Fig. 4. In this example the recombination coefficient was assumed to vary as $T_e^{-3/2}$ ($\hat{k}_r^e = -\frac{3}{2}$) while the electron temperature dependence of the attachment coefficient for CO_2 corresponds to a \hat{k}_{a_1} value which decreases from 45 at $x=0$ at which point $T_e = 0.65$ eV to a value of 3 at $x=20$ at which point $T_e = 1.0$ eV. At the onset of attachment instability ($x \sim 5$ cm) $\hat{k}_{a_1} \sim 30$, $n_n/n_e \sim 0.05$, and the loss of electrons due to attachment is approximately 10% as large as the recombination loss.

tive electron attachment to CO_2 was also included. Near the entrance of the discharge recombination controls electron loss completely and the electron driven thermal instability occurs for ϕ near 90° with a growth rate nearly equal to that of Fig. 5. Unlike the situation in Fig. 5 the thermal instability growth rate in this example decreases in the direction of flow. The reason for the decrease in ν_k is the slight increase in E/n in the flow direction due to gas heating, which leads to a very large increase in k_{a_1} since $\hat{k}_{a_1} \gg 1$ for CO_2 . Such a stabilizing influence when $\hat{k}_{a_1} > 0$ is suggested by the form of Eq. (20), with $\phi = 90^\circ$. Although in this example the loss of electrons due to attachment is increasing rapidly in the first few cm of the discharge, attachment loss is only 10% as large as the recombination loss at about the 5-cm point. Nonetheless, because $\hat{k}_{a_1} \gg 1$ for CO_2 , the conditions for attachment instability are readily satisfied in the direction aligned with the steady field ($\phi = 0^\circ$) at about this location. Thus, while the thermal mode tends to be stabilized by the effect of attachment when $\hat{k}_{a_1} > 0$, attachment instability appears. It is interesting to note that in the 10–15-cm range for which the attachment instability growth rate reaches a maximum, recombination still accounts for approximately half the electron loss.

Because the growth time ($\tau_k \equiv \nu_k^{-1}$) for attachment instability in this example reaches a value which is very much less than the gas residence time in the discharge region, there is ample time for a transition to a new plasma state to occur. Therefore, it is anticipated that plasma characteristics would be altered substantially for the conditions of this example as attachment instability develops. Indeed, experimental evidence shows that running striations occur accompanied by significant changes in average current-voltage characteristics as a consequence of this instability, even though the plasma is likely to remain diffuse.^{8,14,15} For this reason both the zeroth-order (steady) and first-order (stability) characteristics computed using the present model are clearly incorrect for downstream locations beyond about 8 cm in Fig. 7 for which the instability growth time is much less than the residence time remaining. However, the following qualitative observations can be made. As regards electron driven thermal instability, a strong positive electron temperature dependent attachment rate exerts a stabilizing influence in the absence of detachment by decreasing the electron density disturbance. Note that for the indicated point in Fig. 7 at which the contribution of avalanche ionization is 1% as large as the external source, the thermal mode is stable in this case and there is no indication of the effect of avalanche ionization because of the dominant influence of

attachment. Further, in spite of the likelihood of a significant change in plasma conditions when attachment instability occurs, it is clear that the gas will continue to be heated as it is convected through the discharge. Thus, E/n and T_e will increase and a downstream point may be reached for which the conditions for attachment instability are no longer satisfied.⁸ In fact this explains the decrease in the attachment instability growth rate beyond about 15 cm in Fig. 7. Eventually this mode may be stabilized and the thermal mode may reappear as indicated, due primarily to the influence of avalanche ionization which represents about 25% of the total by the 20 cm point for this example.

D. Strong detachment of negative ions

In the preceding discussion attachment was considered only in light of its influence as an electron loss process, without regard to the fate of the negative ions so produced. However, the computed steady-state conditions corresponding to previously examined cases show that the negative-ion concentration can reach a level comparable to and even exceeding that of the electrons when ion-ion recombination is taken as the only loss process for negative ions. It is found experimentally that the presence of high concentrations of negative ions ($n_n/n_e \geq 0.1$) correlates very well qualitatively with the onset of discharge arcing and/or glow collapse.⁹ Negative ions produced either by dissociative attachment involving a primary constituent such as CO_2 or an impurity, subsequently cluster to form very stable species of negative ions.^{9,11-13} While the exact species which dominate are not known, many stable negative-ion species are likely to have detachment rates which are strong functions of gas temperature (and possibly vibrational temperature as well) in the temperature range common to subsonic convection discharges (200–500 °K).

In order to assess the potential influence on thermal instability of negative-ion detachment, two cases were considered. One in which negative ions were produced by a process assumed to have an attachment rate coefficient with a $T_e^{-3/2}$ dependence, i.e., $\hat{k}_{a1} = -\frac{3}{2}$ as in Fig. 5, and a second in which negative ions were produced by dissociative attachment to CO_2 as in Fig. 7. To illustrate the effect of detachment, the detachment coefficient \hat{k}_d was assumed to be that of O_2^- , one of very few negative ions for which the temperature dependence of the detachment process is known.²² In fact, the detachment coefficient for O_2^- exhibits a very strong dependence on gas temperature, e.g., $\hat{k}_d > 10$.

Figure 8 shows the thermal instability growth

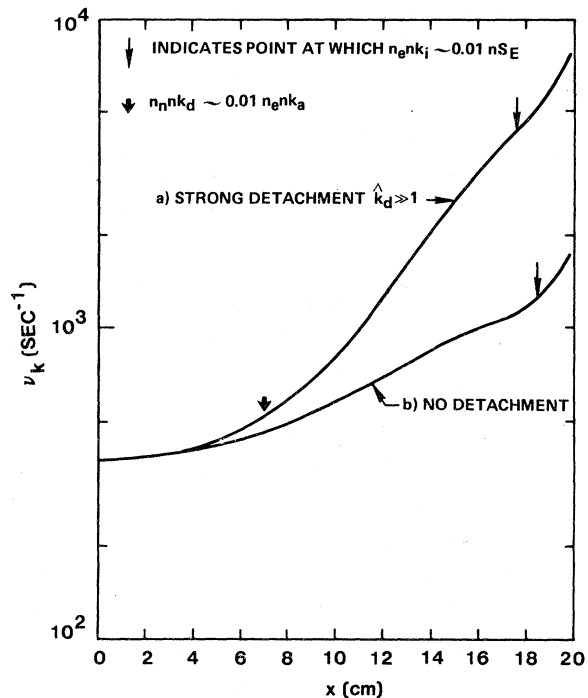


FIG. 8. Computed thermal instability growth rate ($\varphi = 90^\circ$) with and without temperature-dependent detachment of negative ions. The electron temperature dependence of the attachment rate was taken at $T_e^{-3/2}$ ($\hat{k}_{a1} = -\frac{3}{2}$) as in Fig. 5. In this example the dependence of the detachment rate on gas temperature was taken as that of O_2^- corresponding to a \hat{k}_d value which decreases from 30 at $x=0$ ($T=300^\circ\text{K}$) to 10 at $x=20$ cm ($T \approx 700^\circ\text{K}$). In the 6–8-cm range for which detachment first influences the growth rate, $\hat{k}_d \sim 16$ and $n_n/n_e \sim 1$.

rate for the electron driven mode computed with $\hat{k}_{a1} = -\frac{3}{2}$ for plasma conditions generally the same as those discussed previously. Near the discharge inlet ($x \sim 0$) the negative-ion and electron concentrations are about equal having a value of approximately 10^{11} cm^{-3} for this case as shown in Fig. 9. In the absence of detachment both the electron and negative-ion concentrations are essentially independent of position and the instability growth rate rises gradually due to the temperature-dependent reduction in the V - T relaxation time as discussed previously. In this case negative ions are lost by ion recombination alone. However, when detachment having a strong temperature dependence is considered, the instability growth rate begins to rise, reflecting the release of electrons due to detachment. At the 7-cm point at which the growth rate begins to increase noticeably due to detachment, loss of negative ions by way of detachment is only 1% as large as the ion-ion recombination loss. By 15 cm the growth rate is substantially increased even though recombination still domin-

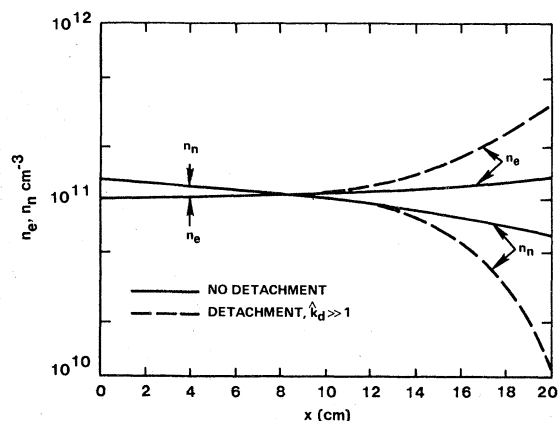


FIG. 9. Computed steady-state electron and negative-ion densities corresponding to the conditions of Fig. 8. Note that in the 6–8-cm range for which detachment first begins to exert a significant influence on the thermal instability growth rate there is no observable reduction in the negative-ion concentration.

ates negative-ion loss and there has been no substantial reduction in negative-ion concentration (Fig. 9). As in previous examples, the predicted steady-state characteristics remain relatively unaffected in comparison to the changes in the instability growth rate.

The trend exhibited by the data of Fig. 8 can be explained simply by examining the response of the electron density disturbance with and without temperature dependent detachment. Figure 10 shows $(n_{e_k}/n_e)(T_k/T)^{-1}$ corresponding to the conditions of Fig. 8. These data show a very large rise in the electron density disturbance as a consequence of temperature-dependent detachment. However, it is interesting to note that by $x \sim 17$ cm, $(n_{e_k}/n_e)(T_k/T)^{-1}$ begins to decrease. This effect occurs in the region at which detachment begins to reduce the negative-ion concentration substantially as shown in Fig. 9. Only the onset of avalanche ionization starts to reverse this trend for the conditions of the present example. Interpretation of the results presented in Figs. 8–10 shows that detachment will exert a strong destabilizing effect when the following two conditions are met: (1) the detachment rate typical of the initial gas temperature is very small permitting a high negative-ion concentration to build up ($n_n/n_e \geq 1$); and (2) the detachment rate has a very strong positive dependence on gas temperature reaching a level such that detachment can begin to free electrons before the end of the discharge region. Such behavior is likely to be typical of detachment of negative ions having moderate binding energies on the order of 1 eV,^{22,23} a value much greater than kT/e but low enough so that detachment can occur in the higher temperature regions of convection discharges.

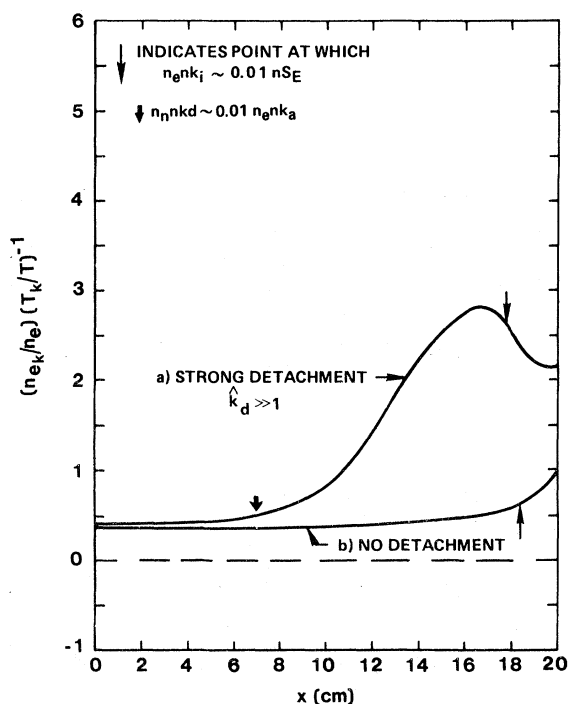


FIG. 10. Computed fractional electron density disturbance relative to a disturbance in gas temperature corresponding to the thermal instability growth rates of Fig. 8.

Clearly the results of Fig. 7 for which attachment instability and thermal instability both occur will also be altered by the onset of detachment. Figure 11 shows computed thermal and attachment instability growth rates for conditions otherwise the same as those in Fig. 7. The interpretation of the various regions in Fig. 11 is the same as that discussed in connection with Fig. 7, but there are several important quantitative differences. Transition from thermal instability to attachment instability occurs at about the same downstream location as in the absence of detachment (Fig. 7). However, the onset of detachment with increasing temperature reduces the negative-ion density substantially compared to the no-detachment case as shown in Fig. 12. Accompanying this reduction in negative-ion density there occurs a decrease in the attachment instability growth rate by about an order of magnitude. The rapidly decreasing negative-ion density results in a compression of the spatial region within which the attachment mode is unstable, with the result that the time required for the gas to pass through the zone of attachment instability is comparable to the instability growth time. Thus, when detachment is important, in some cases there may be insufficient time for a fully developed striated plasma to occur. More importantly, because of the reduced influence of

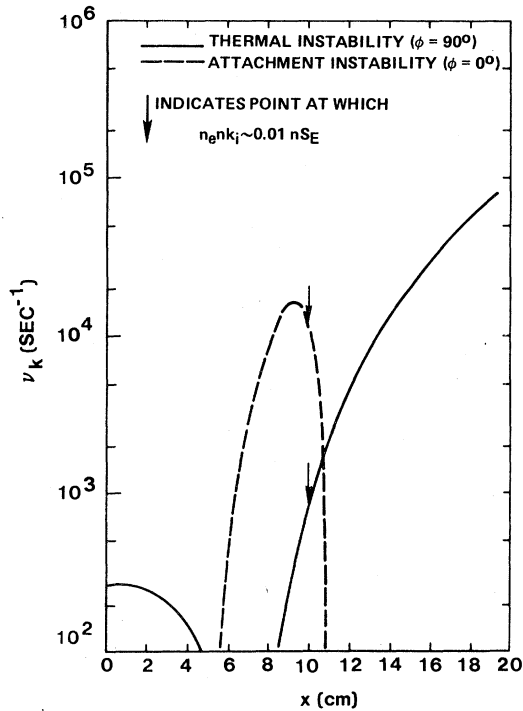


FIG. 11. Computed growth rates for thermal instability ($\phi = 90^\circ$) and attachment instability ($\phi = 0^\circ$) including the effect of temperature-dependent detachment for conditions otherwise the same as those in Fig. 7.

attachment, for the conditions of this example the electron driven thermal mode at $\phi = 90^\circ$ reappears downstream with a very large growth rate at nearly the point for which avalanche ionization constitutes 1% of the total electron production.

The trends exhibited by the data of Fig. 11 are better appreciated upon examination of the fractional electron density disturbance shown in Fig. 13 for $\phi = 90^\circ$. These data vividly illustrate that the first-order response of the plasma to a disturbance can be highly nonuniform spatially although the *predicted* steady state is relatively uniform. For this example, in the $x = 0$ to 3 cm range the relative electron density disturbance $(n_{e_k}/n_e) \times (T_k/T)^{-1}$ is determined by the electron recombination process ($\hat{k}_r^e = -\frac{3}{2}$); dissociative attachment to CO_2 (with $\hat{k}_{a1} \gg 1$) causes a decrease in $(n_{e_k}/n_e)(T_k/T)^{-1}$ between $x = 3$ and 7 cm, until detachment of electrons begins to drive $(n_{e_k}/n_e)(T_k/T)^{-1}$ upward at 7 cm. By 10 cm the onset of avalanche ionization leads to a very large increase in the electron density disturbance.

It is especially interesting to note that the conditions responsible for the extreme spatial variations in the transient response of electron density disturbances as revealed by the data of Fig. 13 have relatively little effect on the predicted steady-state electron density which remains sensibly

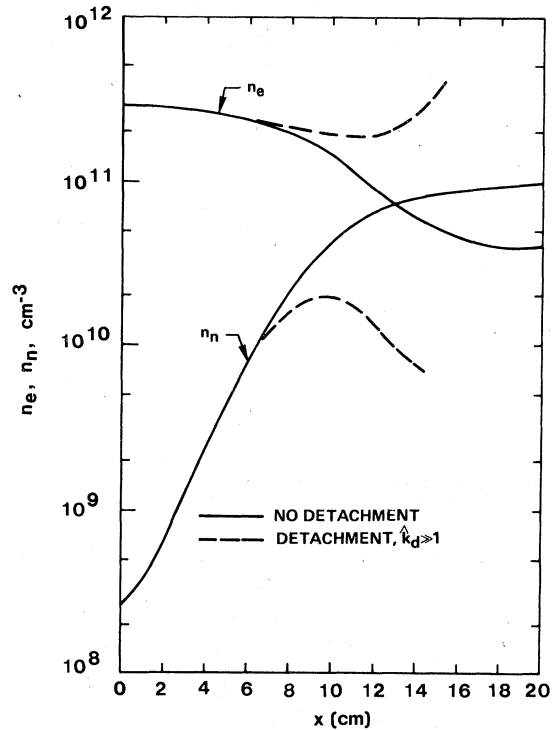


FIG. 12. Spatial variation of electron and negative ion densities corresponding to the conditions of Fig. 7 (no detachment), and Fig. 11 (strong temperature-dependent detachment). These data should be typical of CO_2 laser mixtures for which negative ions are produced only by way of CO_2 dissociative attachment.

constant over most of the region (Fig. 12). Indeed Fig. 14, showing the respective fractional contributions to the loss of electrons, indicates that the minimum contribution of recombination to the total steady-state electron loss is never less than 70% even though the transient response of the plasma is dominated by negative-ion processes. This shows that the importance of negative-ion processes on discharge behavior may be greatly underestimated by relying on simple analysis of the relationship between discharge current density, electric field, and the intensity of the external ionization source.

E. Vibrational reservoir collapse

In each of the preceding examples the driving process for thermal instability was the increase in electron-molecule vibrational excitation in response to a perturbation, a phenomenon in which the vibrational temperature first begins to rise during the initial phase of disturbance growth. However, in Sec. III it was pointed out that because of the high degree of nonequilibrium between vibration and translation the potential exists for a mode

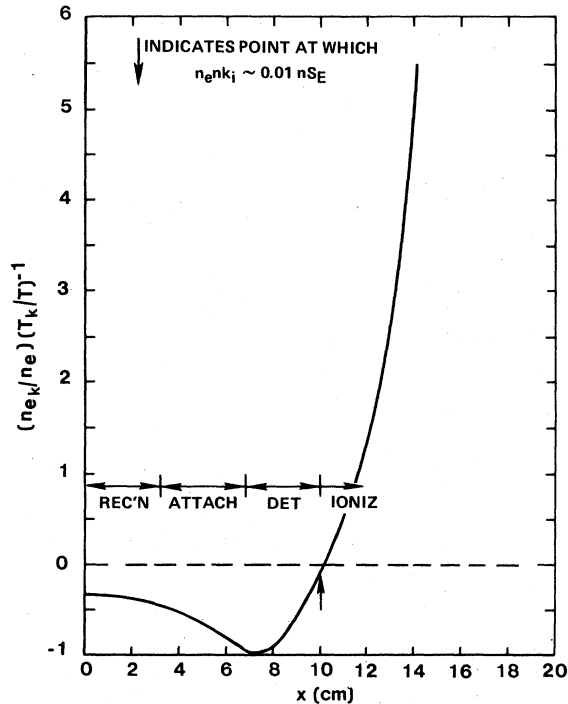


FIG. 13. Fractional electron density disturbance in the direction normal to the steady electric field ($\phi = 90^\circ$) relative to a disturbance in gas temperature for the conditions of Fig. 11. The electron and negative-ion processes dominating the electron density disturbance in various regions are indicated in the figure.

of thermal instability associated with a sharp decrease in T_v , i.e., vibrational reservoir collapse.¹⁷ Such a vibrational relaxation instability is essentially independent of electron properties. Indeed, Eq. (24) indicates that a *necessary* condition for its occurrence in the absence of pressure disturbances is a V - T rate coefficient which increases more strongly than the second power of the gas temperature. This is a direct consequence of the fact that V - T heating of the gas is proportional to the square of the neutral number density. Thus, in order for a local increase in gas translational *energy density* due to V - T relaxation to occur, the V - T rate coefficient must have a temperature dependence strong enough to overcome the tendency of particles to leave the region of increased temperature.

1. V - T rate coefficient

The effective weighted V - T rate coefficient²⁴ for the CO_2 laser mixture used in the previous calculations is presented in Fig. 15. For this example the fractional derivative \hat{k}_{VT} equals 2 at a temperature of about 430 °K and increases rapidly for higher temperatures. However, the rate coef-

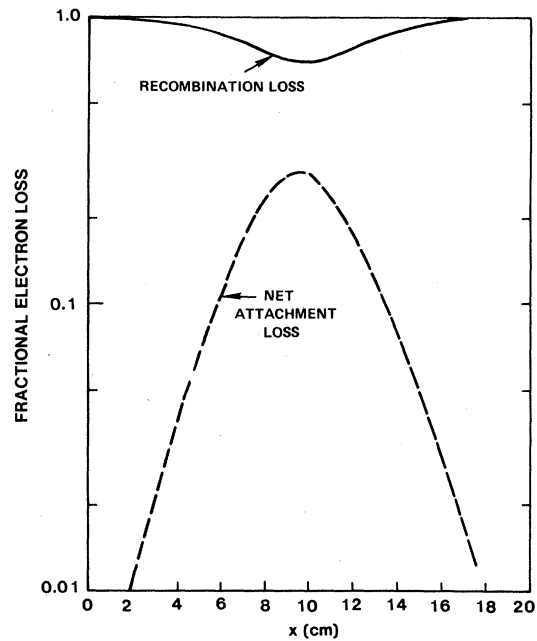


FIG. 14. Relative contributions to the loss of electrons by recombination and the net effect of attachment-detachment kinetics. Note that although negative-ion processes exert the dominant influence on the evolution of plasma disturbances (Figs. 11 and 13), as regards predicted steady-state characteristics the plasma differs only slightly from the case in which recombination is the only loss.

ficients for V - T relaxation in gases can vary greatly²⁴ and are not always well known, particularly if V - T relaxation by impurities is important. For these reasons the precise temperature dependence of V - T rate coefficients are seldom known. In order to evaluate vibrational reservoir collapse as a potential cause of thermal instability in high power discharges, numerical variation of the temperature dependence of the V - T rate coefficient was carried out. For comparison Fig. 15 shows a trial V - T rate coefficient which is proportional to the fourth power of gas temperature over the entire range, i.e., $\hat{k}_{VT} = 4$ for all T values. This trial function differs from the mixture weighted function by no more than a factor of 2 in the 300–600 °K range.

Using these V - T rate coefficients along with plasma conditions similar to those described previously, the growth rates for thermal instability were computed for a recombination dominated plasma ($\hat{k}_r^e = -\frac{1}{2}$); results are presented in Fig. 16 for the direction normal to the direction of the electric field, $\phi = 90^\circ$. The interpretation of the data obtained using the mixture weighted k_{VT} function is generally the same as that discussed in connection with the data of Fig. 5. In this case the

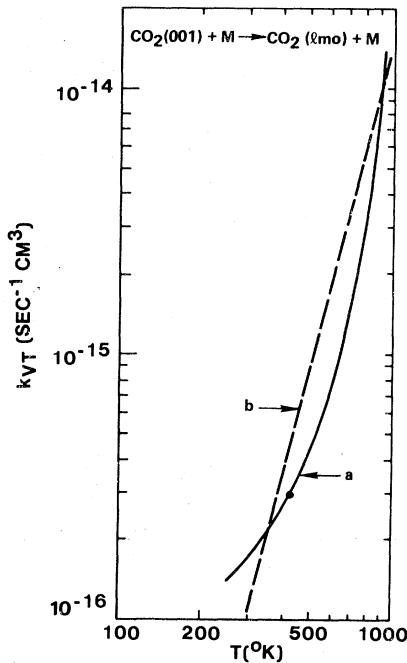


FIG. 15. Vibrational relaxation coefficient for the process $\text{CO}_2(001) + M \rightarrow \text{CO}_2(lm0) + M$, mixture weighted for $\text{CO}_2\text{-N}_2\text{-He}$ in the proportions 0.05-0.35-0.60 so as to be consistent with the diatomic gas approximation described in Sec. IV A, curve a; also shown is a trial V - T rate coefficient proportional to the fourth power of temperature ($\hat{k}_{VT}=4$), curve b. The symbol \bullet on curve a indicates the temperature for which $\hat{k}_{VT}=2$. In the present analysis this process is assumed to result in instantaneous gas heating and therefore this rate coefficient is the effective V - T relaxation rate coefficient.

electron vibrational pumping dominates resulting in the electron driven thermal mode discussed previously. The growth rate of this mode increases with increasing downstream temperature due to the enhanced feedback by way of the V - T relaxation process. In striking contrast, the stronger temperature dependence of the trial k_{VT} function at the discharge inlet temperature (300°K) leads to vibrational reservoir collapse accompanied by an order-of-magnitude increase in the instability growth rate. Figure 17 shows that the thermal instability growth rate is nearly isotropic when this occurs. This reflects the fact that vibrational relaxation which is isotropic, rather than electron pumping which is not, is the fundamental initiating mechanism for this instability.¹⁷ Moreover, although k_{VT} increases with temperature in both examples, as temperature rises with downstream position Fig. 16 shows that the growth rate of this mode actually decreases unlike the electron driven mode. Since, vibrational reservoir collapse leads to a decrease in T_v during a disturbance, increased V - T relaxation tends to re-

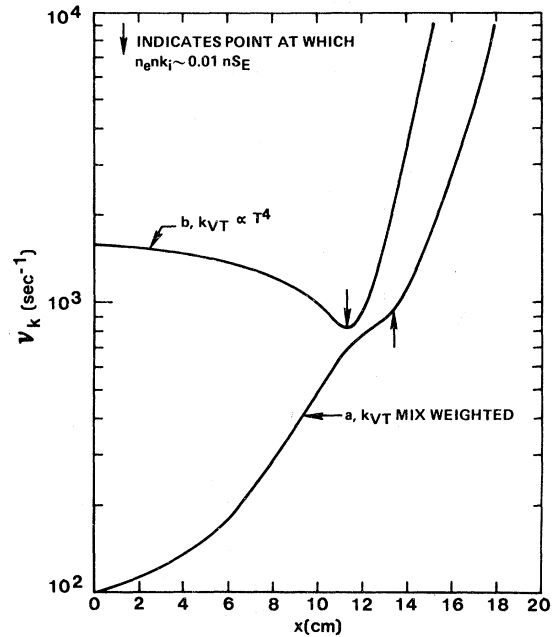


FIG. 16. Thermal instability growth rates in the direction normal to the steady electric field ($\phi = 90^\circ$) computed using the V - T rate coefficients of Fig. 15 for plasma conditions generally similar to those of Figs. 4 and 5.

duce the degree of nonequilibrium between translation and vibration, thereby exerting a stabilizing influence on this mode. This effect is reflected in the form of Eq. (24) which shows that as τ_{VT} decreases the growth rate decreases at sensibly constant power density.

2. Vibrational temperature disturbances

The spatial dependences of all computed steady plasma properties (including vibrational temperature) obtained using the two rates coefficients of Fig. 16 differed by less than 10% over the first 10 cm of the discharge reflecting the nearly equal magnitudes of k_{VT} . However, the response of the competing processes tending to maintain the vibrational temperature at a level between the electron and gas temperature varies markedly in the two examples. This is vividly illustrated by the fractional response of vibrational temperature to a change in gas temperature as shown in Fig. 18. For the electron driven vibrational mode $(T_{v_k}/T_v)(T_k/T)^{-1}$ is positive reflecting the dominance of electron vibrational excitation over V - T relaxation during a disturbance. Even in this case the magnitude of $(T_{v_k}/T_v)(T_k/T)^{-1}$ decreases rapidly with downstream position. This trend is a consequence of the fact that \hat{k}_{VT} increases rapidly with T for the mixture weighted k_{VT} coefficient and exceeds 2 for $T \sim 430^\circ\text{K}$. When $\hat{k}_{VT}=4$ over the en-

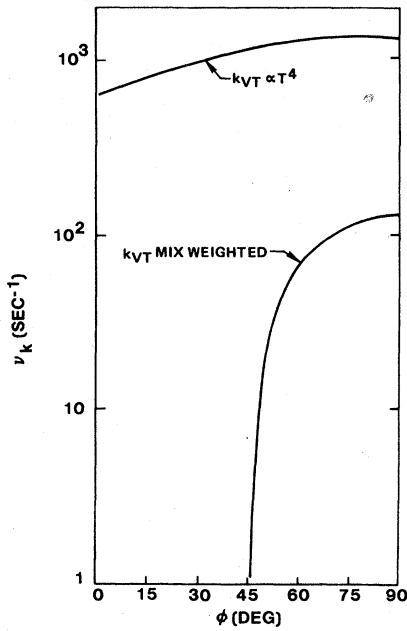


FIG. 17. Dependence of thermal instability growth rates on spatial orientation relative to the direction of the steady electric field corresponding to the data of Fig. 16 for $x = 4$ cm.

tire temperature range, a condition resulting in the vibrational relaxation mode of instability, $(T_{v_k}/T_v)(T_k/T)^{-1}$ is negative indicative of vibrational reservoir collapse until the location is reached for which avalanche ionization becomes

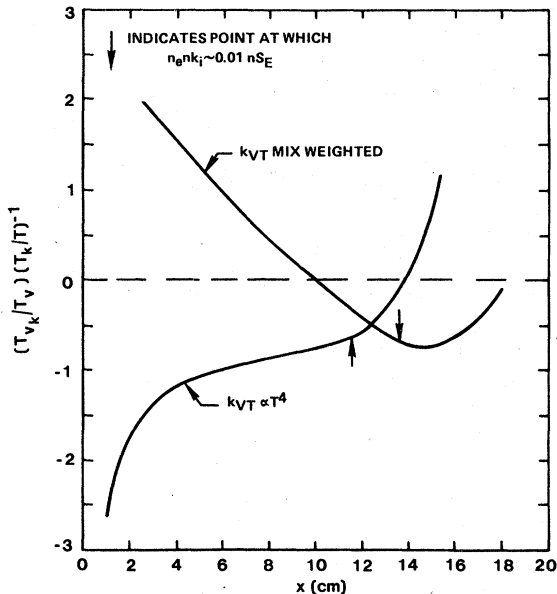


FIG. 18. Fractional disturbance in vibrational temperature relative to a change in gas temperature corresponding to the growth rates of Fig. 16.

important. At this point electron vibrational pumping again dominates the vibrational temperature response and $(T_{v_k}/T_v)(T_k/T)^{-1}$ begins to rise rapidly.

On the basis of these results the following observations can be made. Collapse of the vibrational reservoir *can* occur in externally sustained discharges when (1) the V - T relaxation rate is small resulting in a high degree of vibrational-translational nonequilibrium; and (2) the V - T rate coefficient has a strong positive dependence on temperature allowing a disproportionate increase in V - T energy relaxation in response to a local positive temperature perturbation. The marked differences in the results presented in Figs. 16-18 provide further evidence of the fact that seemingly minor changes in the dependence of a rate coefficient on its primary variable can drastically alter the transient response of the plasma to a disturbance even though the predicted steady state remains essentially unchanged.

V. SUMMARY

Based on the results presented in the preceding sections it can be concluded that externally sustained discharges of the type used in CO_2 and CO laser applications are inherently unstable, and that the growth rate of thermal instability is exceptionally sensitive to the electron loss process. The results presented here show that convective removal of the unstable plasma from the discharge region before glow collapse and/or arcing can occur accounts for the ability to maintain apparently stable cw glow discharges at high pressure.^{5,6,25}

A primary reason for employing external, independently controllable means for plasma production is the extreme sensitivity of low energy electron impact ionization to electron temperature variations. The results presented here show that because of this sensitivity avalanche ionization can significantly affect the onset of thermal instability even though the contribution of this process to steady-state electron production may only be 1% as large as that of the external source. This finding suggests that the premature onset of avalanche ionization in high-current-density regions near electrodes and in boundary layers will become an important factor contributing to thermal instability for plasma conditions such that the inferred *average* steady-state properties would be entirely unaffected.

This analysis also shows that very small differences in the specific nature of the *electron loss process* can cause order-of-magnitude variations in the thermal instability growth rate. In fact, the magnitude of the first-order electron density dis-

turbance has been found to exhibit much greater variation in externally sustained discharges than in otherwise similar self-sustained discharges. For this reason the transient response to disturbances of externally sustained plasma properties is likely to be highly nonuniform even though the predicted zeroth-order (steady-state) properties may be sensibly uniform.

Externally sustained CO₂ and CO laser discharges are generally operated at relatively high pressure (≥ 0.1 atm) and low translational temperatures (≤ 300 °K). Under these conditions both positive and negative ions are likely to be clustered.¹³ Unfortunately, the dependence of the recombination coefficients on both electron temperature and gas temperature for such ion species

are generally unavailable. In addition, the dependence of electron detachment from stable negative ions on both translational and vibrational temperature is unknown. The present results suggest that this process may impact significantly on thermal instability growth rates in externally sustained plasmas. Clearly there is a need for basic data relevant to cluster-ion loss processes for the discharge conditions described herein.

ACKNOWLEDGMENTS

It is a pleasure to acknowledge the expert assistance of E. J. Seligman and J. R. Caspar, who were responsible for the programming and numerical work. Also, the continued interest of R. H. Bullis and W. J. Wiegand is much appreciated.

*Work performed in part through the sponsorship of the Office of Naval Research.

¹C. A. Fenstermacher, M. J. Nutter, W. T. Leland, and K. Boyer, *Appl. Phys. Lett.* **20**, 56 (1972); J. P. Reilly, *J. Appl. Phys.* **43**, 3411 (1972); O. R. Wood, *Proc. IEEE* **62**, 355 (1974); and J. D. Daugherty, in *Principles of Laser Plasmas*, edited by G. Bekefi (Wiley, New York, 1976).

²E. P. Velikhov, S. A. Golubev, Yu. K. Zamtsov, A. F. Pal', I. G. Persiantsev, V. D. Pis'mennyi, and A. T. Rakhimov, *Zh. Eksp. Teor. Fiz.* **65**, 543 (1973) [*Sov. Phys.-JETP* **38**, 267 (1974)].

³E. P. Velikhov, S. A. Golubev, A. S. Kovalev, I. G. Persiantsev, V. D. Pis'mennyi, and A. T. Rakhimov, *Fiz. Plazmy* **1**, 847 (1975) [*Sov. J. Plasma Phys.* **1**, 463 (1975)].

⁴L. P. Menakhin, E. K. Eroshchenkov, and K. N. Ul'yanov, *Zh. Tekh. Fiz.* **45**, 1346 (1975) [*Sov. Phys.-Tech. Phys.* **20**, 851 (1976)].

⁵W. L. Nighan and W. J. Wiegand, *Appl. Phys. Lett.* **25**, 633 (1974).

⁶W. L. Nighan, in *Principles of Laser Plasmas*, edited by G. Bekefi (Wiley, New York, 1976), and references cited therein.

⁷R. A. Haas, *Phys. Rev. A* **8**, 1017 (1973), and references cited therein.

⁸W. L. Nighan and W. J. Wiegand, *Phys. Rev. A* **10**, 922 (1974), and references cited therein.

⁹H. Shields, A. L. S. Smith, and E. Norris, *J. Phys.* **D 9**, 1587 (1976).

¹⁰W. L. Nighan, *Phys. Rev. A* **2**, 1989 (1970).

¹¹W. J. Wiegand and W. L. Nighan, *Appl. Phys. Lett.* **22**, 583 (1973).

¹²J. F. Prince and A. Garscadden, *Appl. Phys. Lett.* **27**, 13 (1975).

¹³H. W. Ellis, R. Y. Pai, I. R. Gatland, and E. W. McDaniel, *J. Chem. Phys.* **64**, 3935 (1976).

¹⁴D. H. Douglas-Hamilton and S. A. Mani, *Appl. Phys. Lett.* **23**, 508 (1973).

¹⁵D. H. Douglas-Hamilton and S. A. Mani, *J. Appl. Phys.* **45**, 4406 (1974).

¹⁶A. S. Kovalev, I. G. Persiantsev, V. D. Pis'mennyi, and A. T. Rakhimov, *Phys. Lett.* **49A**, 29 (1974).

¹⁷A. V. Eletski and A. N. Starostin, *Fiz. Plazmy* **1**, 684 (1975) [*Sov. J. Plasma Phys.* **1**, 377 (1975)].

¹⁸E. P. Velikhov, I. V. Novobrantsev, V. D. Pis'mennyi, A. T. Rakhimov, and A. N. Starostin, *Dokl. Adad. Nauk. SSSR* **205**, 1328 (1973) [*Sov. Phys.-Dokl.* **17**, 772 (1973)].

¹⁹J. H. Jacob and S. A. Mani, *Appl. Phys. Lett.* **26**, 53 (1975).

²⁰E. F. Jaeger, L. Oster, and A. V. Phelps, *Phys. Fluids* **19**, 819 (1976).

²¹J. L. Pack and A. V. Phelps, *J. Chem. Phys.* **44**, 1870 (1966).

²²J. L. Pack and A. V. Phelps, *J. Chem. Phys.* **45**, 4316 (1966).

²³J. N. Bardsley and M. A. Biondi, in *Advances in Atomic and Molecular Physics*, edited by D. R. Bates (Academic, New York, 1970), Vol. 6; also see M. A. Biondi, in *Principles of Laser Plasmas*, edited by G. Bekefi (Wiley, New York, 1976).

²⁴R. L. Taylor and S. Bitterman, *Rev. Mod. Phys.* **41**, 26 (1969).

²⁵The extension of this conclusion to the discharge duration time in pulsed discharges is straightforward.